Photopyroelectric study of specific heat, thermal conductivity, and thermal diffusivity of Cr_2O_3 at the Néel transition

M. Marinelli,* F. Mercuri, U. Zammit, R. Pizzoferrato, and F. Scudieri
Dipartimento di Ingegneria Meccanica, 2° Università di Roma "Tor Vergata," Via della Ricerca Scientifica, 00133 Roma, Italy

D. Dadarlat
Institute of Isotopic and Molecular Technology, P. O. Box 700, Cluj-Napoca 5, R-3400 Romania
(Received 28 June 1993; revised manuscript received 12 November 1993)

A photopyroelectric technique has been used to simultaneously measure the critical behavior of specific heat, thermal conductivity, and thermal diffusivity of Cr_2O_3 at the antiferromagnetic-paramagnetic phase transition. An Ising-like behavior has been found for $|t_{max}| \leq 3\times10^{-3}$ with $\alpha=0.10\pm0.02$ and $A/A'=0.48\pm0.03$. A possible crossover between Ising and Heisenberg behaviors has been found if $|t_{max}|$ is increased. Thermal diffusivity data have been fitted according to the model for uniaxial antiferromagnet with energy conservation for $|t_{max}| \leq 3\times10^{-3}$ with a critical exponent $b=-0.11\pm0.02$. A correction term similar to the static correction to scaling factor has been introduced in the fitting function. No anomaly has been found in thermal conductivity.

I. INTRODUCTION

The critical phenomena associated with thermal parameters at magnetic phase transitions has been widely studied in the past. Most of the experimental results seem to confirm the universality hypothesis which states that the critical behavior depends only on the dimensionality of the system (d) and on the degree of freedom of the order parameter (n). An antiferromagnet, for example, provided that only short-range interactions are relevant in the system can be described by a Heisenberg model if $d=3$ and $n=3$ or by an Ising one if $d=3$ and $n=1$. There are systems, however, which do not seem to follow the universal behavior and many possible explanations have been suggested. In the case of specific-heat data, Ahlers and Kornblitt[1] for example, argue that the disagreement could be due to the presence of long-range interactions like the dipole-dipole ones which in some materials can be relevant. In this case a crossover from the Heisenberg behavior to a mean-field one very close to T_c could be observed. Bruce and Cannel,[2] on the other hand, try to explain the deviation of their results on the specific heat from universality at the antiferromagnetic-paramagnetic phase transition in Cr_2O_3 with a systematic error which is due to the fact that while the theoretical predictions are valid for the specific heat at constant volume, the measurement is performed at constant pressure. This could be a severe limit in the interpretation of the results especially in system with a large expansion coefficient.

It should be noted that while very many data are available in literature for the critical behavior of static quantities such as the specific heat, the situation is completely different in the case of dynamic quantities like the thermal diffusivity and the thermal conductivity. There are few high-resolution data which can be used to study in detail the dynamic critical behavior. Apart from the superfluid transition in He (Ref. 3) and some recent results at various transitions in liquid crystals,[4] to our knowledge no data on the critical behavior of the thermal diffusivity and thermal conductivity have been reported. It is a worthwhile to note that the results on the critical behavior of dynamic quantities can greatly help also in the understanding of the open questions connected to a given transition.

In the present paper, high-resolution simultaneous measurements of specific heat, thermal diffusivity, and thermal conductivity of Cr_2O_3 are reported. Cr_2O_3 is a weakly anisotropic antiferromagnet which is expected to follow a Heisenberg behavior and perhaps an Ising one close to T_c. Our specific-heat data show an Ising-like behavior for $|t| \leq 3\times10^{-3}$ with a possible crossover to Heisenberg if a wider temperature range is considered in the fit. No singular behavior but a change in slope and a small discontinuity at T_c have been obtained for the thermal conductivity. The thermal diffusivity data, which show a dip at T_c, can be interpreted, in the reduced temperature range $|t| \leq 3\times10^{-3}$, using a dynamic model corresponding to a uniaxial antiferromagnet with energy conservation.

II. Cr_3O_3 PROPERTIES

As already stated Cr_2O_3 is a low anisotropy easy-axis antiferromagnet with a Néel temperature at about 307 K. It has a corundum structure with an orthorombic unit cell, the [111] direction of such a unit cell being the c axis which is also the easy axis of magnetization. Inelastic neutron scattering has been used to study spin waves at 78 K (Ref. 5) and exchange constants have been calculated. Such constants are about 20 times larger for near and next neighbor than all the others. Measurements of magnetic susceptibility and antiferromagnetic resonance[6] have shown that the anisotropy field and the exchange field at $T=0$ K are 7×10^2 and 2.45×10^6 Oe, respectively, the ratio of the two ($\sim10^{-4}$) being unusually small for

a uniaxial antiferromagnet. This is the reason why the system could be expected to follow a Heisenberg behavior ($n=3$) and perhaps an Ising one ($n=1$) very close to the transition temperature. Regarding the critical behavior of this system very little is known and the available critical exponents seem not to show any clear evidence of Heisenberg or Ising behavior. Staggered susceptibility[7] has been measured near the Néel temperature and has been reported to diverge with a critical exponent $\gamma=-1.35\pm0.05$ which is in agreement with that predicted by the Heisenberg model. On the other hand, sound velocity attenuation measurements[8] have been interpreted with a specific-heat critical exponent of $\alpha=0.14$, not too far from what is expected for the Ising like behavior. The specific-heat critical exponent has also been measured with a calorimetric technique[2] and the obtained exponent was $\alpha=-0.12$. Although this seems to be in agreement with what is predicted from the Heisenberg model, the authors, on the basis of a detailed statistical analysis of their data, argue that this conclusion can be neither confirmed nor excluded. The argument is based on the presence of a systematic error in the measurement due to an anisotropic thermal expansion coefficient in the vicinity of the transition temperature which is the origin of the systematic error in the comparison between the experimental results (constant pressure) and theoretical predictions (constant volume). In the same paper, thermal conductivity data as a function of temperature have been reported. They show a decrease with a temperature increase with a peak, which has been regarded as an experimental artifact, and a change in slope at the transition temperature.

III. EXPERIMENTAL

The experimental setup used was a standard photopyroelectric configuration.[9] Several Cr_2O_3 slices of about 5 mm in diameter and different thickness have been cut and polished from a $3N$ purity single-crystal ingot. One side of the sample was in thermal contact with a 300-μm-thick $LiTaO_3$ pyroelectric transducer by means of a coupling fluid whose influence on the heat transport process is negligible as will be shown later. The other sample surface was heated by an acousto-optically modulated He-Ne laser. The photopyroelectric signal amplitude and phase were obtained by a two phase lock-in amplifier. It has been shown[10] that if the sample is optically opaque ($\mu_\beta \ll l_s$, where μ_β is the optical penetration depth, l_s is the sample thickness and subscripts s and p refer to the sample and the transducer, respectively), the pyro and the sample are thermally thick ($\mu_{s,p} \ll l_{s,p}$ where $\mu=\sqrt{2D/\omega}$, $D=k/\rho c$ is the thermal diffusivity and ω the angular modulation frequency) and $\beta_s\mu_s \gg 1$, where β_s is the sample absorption coefficient, then,

$$|V(\omega)|=\frac{I_0\eta_s AR}{l_p[1+(\omega\tau_e)^2]^{1/2}}\frac{p}{\rho_p c_p}\frac{e^{-\sqrt{\omega/2D}\,l_s}}{e_s(e_p/e_s+1)}, \quad (1)$$

$$\phi(\omega)=-\arctan(\omega\tau_e)-\left[\frac{\omega}{2D}\right]^{1/2} l_s, \quad (2)$$

where I_0 is the nonreflected light source irradiance incident at the sample surface, η_s is the nonradiative conversion efficiency, ρ is the density, $f_e=1/2\pi\tau_e$ is the transducer plus detection electronic cutoff frequency, $e=\sqrt{\rho ck}$ is the thermal effusivity, and c and k are the specific heat and the thermal conductivity, respectively. The sample thermal diffusivity can be calculated from the signal phase and then substituted in the signal amplitude to obtain the sample thermal effusivity. The thermal conductivity and specific heat can be calculated as follows:

$$c_s=e_s/\rho_s\sqrt{D_s}, \quad k_s=e_s\sqrt{D_s}\ .$$

It has been shown[11] that in Cr_2O_3 there is no discontinuity in the volume of the unit cell at T_c and that the thermal expansion is so small that the error we make considering the density as a constant all over the investigated temperature range in the derivation of the specific-heat value is negligible. It is worthwhile to note that with the present technique the critical behavior of static and dynamic quantities can be studied on the same sample under the same experimental condition, such as thermal gradients, heating rate, etc., and that would be very helpful when using the results of the measurements in scaling laws.

We used a negative lens to spread the light on a larger area with respect to the beam diameter so as to control the power density impinging on the specimen. In all the experiments the illuminated area of the sample was much greater than its thickness to allow a one-dimensional approach for which Eqs. (1) and (2) have been obtained. The sample and the transducer were contained in an oven whose temperature rate change was of (4±1) mK/min. Data were collected every 2 mK and the sample temperature was controlled by means of a thermistor. The samples' surfaces have been blackened with a thin layer of carbon black to make sure that no contribution due to possible reflectivity changes are present in the signal. It is well known that a too high power density and a too fast heating rate can affect the results of the measurement, the sample not being in thermal equilibrium. We successively decreased both the heating rate and the power density down to values where a further decrease gave no effects on the measurement. Different measurements at different frequencies in the range 20–80 Hz have been performed: the obtained results for the thermal parameters were the same within the experimental errors. This ensures that there is no effect due to the thermal coupling fluid, which was silicone grease. Several runs have been performed heating the transducer alone to check for a significant variation of its pyroelectric constant and thermal properties in the temperature range 20–60 °C. In agreement with that reported in Ref. 12, no variations were observed provided that the transducer was constraint free. On the other hand, during the measurement the sample itself can act as a constraint for the transducer. We made runs with the sample attached on the opposite sides of the transducer with respect to the heated one and again no variation of the pyroelectric constant and transducer thermal parameters were detected provided that the sample surface was small with respect to the pyro one.

A frequency scan has been performed for each sample

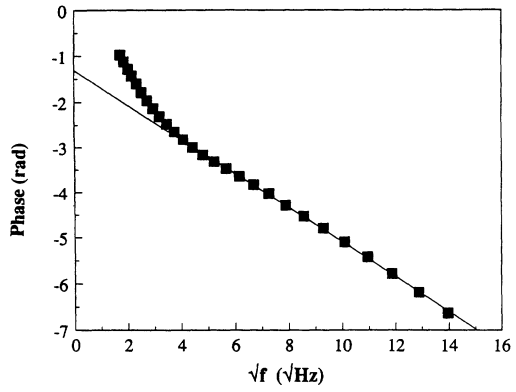

FIG. 1. Photopyroelectric signal phase vs square root of frequency for a 350-μm-thick Cr_2O_3 sample.

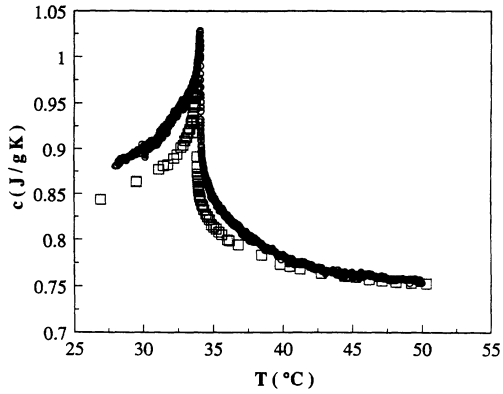

FIG. 2. Specific heat vs temperature: □ data taken from Ref. 2; ○ data obtained from a 350-μm-thick sample.

to experimentally determine the frequency at which the condition for the validity of Eqs. (1) and (2) are fulfilled. In particular, from Eq. (2), a linear dependence of the signal phase vs $\sqrt{f}$ must be expected if $\omega\tau_e \gg 1$. Figure 1 shows the results obtained for a 350-μm-thick sample: a region of linear dependence is clearly evident for frequencies greater than 30 Hz. For such a sample the measurements were performed at 78 Hz. This linear dependence is more experimental evidence that the results are not influenced by the presence of the coupling fluid. Choosing the working frequency well within the linear region of a frequency scan for each measured sample the same behavior of the thermal parameters have been obtained, thus confirming the homogeneity of the ingot from which the samples were cut. A normalization on the amplitude and phase of the signal have been performed using data reported in Ref. 2 for the specific heat and thermal conductivity at 50 °C, which is a temperature away from the transition one so that possible differences in the sample purity and homogeneity are not relevant. This normalization is necessary to make the results dependent only on the sample parameters, the modulation frequency and the pyro thermal effusivity being known. It must be noted that the transition temperature for our samples is always higher than the one reported in Ref. 2 thus denoting a better sample quality. We have also annealed one of our samples in a nitrogen atmosphere at 850 °C for 40 h, allowing it to cool down to room temperature in 24 h to remove possible mechanical stresses that can affect the critical behavior of the thermal parameters. Again the obtained experimental results were similar to the ones obtained in as-grown samples.

IV. EXPERIMENTAL RESULTS

A. Specific heat

Figure 2 shows the results obtained for the specific heat of the 350-μm-thick sample at 78 Hz in the temperature range 29–51 °C compared with the ones reported in Ref. 2. As already stated, the photopyroelectric technique gives relative quantities and, therefore, a calibration is required. In our case we used the values reported by Bruce and Cannell,[2] for the specific heat and thermal conductivity at 50 °C. Differences among samples can be relevant in this calibration procedure, especially in a temperature region close to the transition, where, because of the possible strong temperature dependence of thermal parameters, impurities and crystal imperfections can substantially alter the critical behavior. Since the width at half maximum of the specific heat is less than 2 °C we think that 50 °C is sufficiently far from the transition temperature, which is at about 34 °C, to minimize the effect of the calibration.

There are two main differences between the two sets of data: the peak value is obtained at about 100 mK higher temperature in our sample, thus confirming the good quality of the crystal, and a less rapid decrease on both sides with respect to T_c is clearly evident. Figure 3 shows the results obtained from three different samples: samples b and c were 350 and 520 μm thick, respectively, while sample a is the same as sample c after the annealing procedure already described in experimental section. The modulation frequency was 78 Hz for sample b and 27 Hz for samples a and c. The three curves superimpose one on top of the other but curve a and c in Fig. 3 have been

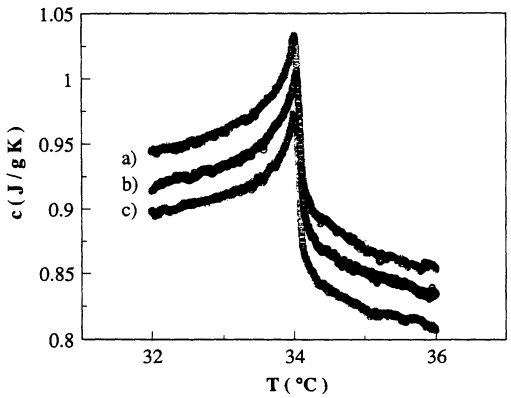

FIG. 3. Specific heat vs temperature: (a) 520-μm-thick sample annealed at 850 °C for 40 h and cooled down to room temperature in 24 h; (b) 350-μm-thick sample; (c) 520-μm-thick sample. The modulation frequency was 78 Hz for sample (b) and 27 Hz for samples (a) and (c). Curves (a) and (c) have been shifted down and up of 0.025 J/gK, respectively.

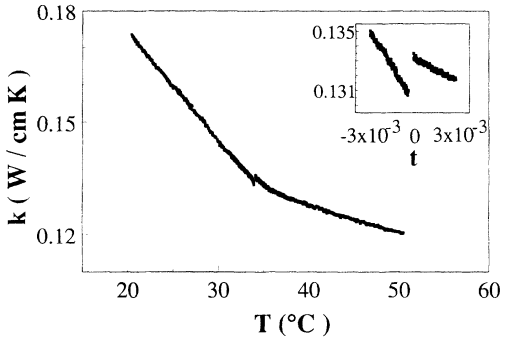

FIG. 4. Thermal conductivity data vs temperature.

shifted, for clarity, down and up a fixed amount, respectively. The comparison between curves b and c demonstrates the reproducibility of the measurements and also the homogeneity of the ingot from which the slices were cut. As already stated, crystal imperfections or strains in the sample can substantially alter the critical behavior. The comparison between curve c and a shows that before and after the annealing no significant changes can be detected. This means that in our Cr_2O_3 samples there is no contribution to the critical behavior from the crystal defects which can be removed with the above mentioned heat treatment.

B. Thermal conductivity and thermal diffusivity

Figure 4 shows the behavior of thermal conductivity. Even if the transition is not as evident as in the case of specific heat, a clear change in slope in the curve and a discontinuity in the vicinity of T_c, shown in the insert, are detectable. The above-mentioned change in slope is also evident in the data reported in Ref. 2 and it seems qualitatively consistent with the one present in our results.

A completely different behavior has been obtained in the vicinity of T_c: while Bruce and Cannell reported a peak which has been attributed to some experimental artifact, a discontinuity which will be discussed later on, is present in our data. A sharp dip, due to "critical slowing down," has been obtained in the thermal diffusivity as shown in Fig. 5. To the best of our knowledge, these are the first thermal diffusivity data, for a magnetic transition, reported in literature.

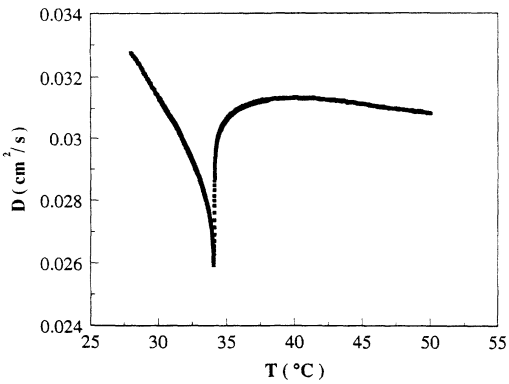

FIG. 5. Thermal diffusivity data vs temperature.

V. DATA ANALYSIS

A. Fitting functions

The critical behavior of the specific heat is generally described by a function of the form

$$C_p=(\bar{A}/\alpha)|t|^{-\alpha}(1+\bar{D}|t|^x)+B+\bar{E}t\ , \tag{3}$$

where $t=(T-T_c)/T_c$, α, $\bar{A}$, $\bar{D}$, B, $\bar{E}$, and T_c are adjustable parameters for $T>T_c$. Primed parameters will be used for $T<T_c$. The linear term represents a regular contribution to the specific heat due to the transition itself. This means that $\bar{E}$ must be equal to $\bar{E}'$. A trivial consequence of the continuity of C_p imposes $B=B'$ if $\alpha<0$. This equality, however, must be valid even for positive α and follows from a more detailed calculation based on the renormalization group (RG). The term $(1+D|t|^x)$ is the correction to scaling term which represents a singular contribution to the leading power if $x=0.5$ as known both from experiments[13] and theory.[14] To reduce the statistical correlation among sets of parameters the expression we have used in our fitting routine was

$$C_p=A|T-T_c|^{-\alpha}(1+D|T-T_c|^x)+B+E(T-T_c)\ . \tag{4}$$

Provided that we consider $|T-T_c|$ as $|(T-T_c)/1K|$, parameters in Eqs. (3) and (4) have the same units, even if the standard errors between the two sets cannot be compared in an easy way. Therefore, the same relations which apply among the parameters in Eq. (3) must also apply to the parameters in Eq. (4). Regarding the thermal diffusivity, the analysis has been made assuming that it is given, similarly to the specific heat, by a sum of a regular term plus a singular one, with a correction term

$$D=V+W(T-T_c)+U|T-T_c|^{-b}(1+F|T-T_c|^x) \quad (\text{with } b<0)\ . \tag{5}$$

The constraint on the exponent b is due to the fact that D cannot diverge at T_c. Correction terms in the thermal transport parameters are sometimes necessary to account for the departure from universality as in the case of liquid He.[15] We used a correction to the scaling factor similar to the one for the specific heat with the same exponent $x=0.5$.[15] The reason for this particular choice will be clear in the following discussion of the results. The thermal conductivity was obtained from the specific heat and thermal diffusivity data.

B. Fitting procedure

Specific-heat data for $T<T_c$ and $T>T_c$ were simultaneously fitted with a nonlinear least-squares routine, initially assuming $D=D'=0$. Regarding the other parameters $B=B'$, $E=E'$, $\alpha=\alpha'$, and $T_c=T_c'$ were the con-

TABLE I. Results of the fit for the specific-heat data with no correction to scaling term.

	Fit 1	Fit 2	Fit 3	Fit 4
t_{max}	5×10^{-3}	8×10^{-3}	5×10^{-3}	3×10^{-3}
t_{min} $(T<T_c)$	3.0×10^{-4}	3.1×10^{-4}	3.3×10^{-4}	3.2×10^{-4}
t_{min} $(T>T_c)$	4.9×10^{-4}	7.5×10^{-6}	2.6×10^{-6}	2.4×10^{-6}
T_c (K)	307.173±0.025	307.264±0.025	307.258±0.025	307.259±0.025
α	−0.043±0.006	−0.12±0.05	−0.046±0.008	−0.0046±0.008
A' (J/gK)	$(-4.6\pm0.1)\times10^{-1}$	$(-2.92\pm0.06)\times10^{-1}$	$(-6.67\pm0.06)\times10^{-1}$	$(-6.79\pm0.06)\times10^{-1}$
A (J/gK)	$(-5.5\pm0.1)\times10^{-1}$	$(-1.27\pm0.06)\times10^{-1}$	$(-3.21\pm0.06)\times10^{-1}$	$(-3.18\pm0.06)\times10^{-1}$
E (J/gK)	$(-5.8\pm3.0)\times10^{-3}$	$(-5.6\pm0.8)\times10^{-3}$	$(-3.4\pm0.8)\times10^{-3}$	$(-3.3\pm0.8)\times10^{-3}$
B' (J/gK)	1.40±0.01	1.22±0.01	1.60±0.01	1.61±0.01
B (J/gK)	1.40±0.01	$(9.8\pm0.1)\times10^{-1}$	1.17±0.01	1.17±0.01
A/A'	1.20±0.05	0.43±0.03	0.48±0.02	0.47±0.02
rms	0.00155	0.00179	0.00149	0.00148

straints used during the fit. First we made a rough estimation from the data plot of the region affected by the rounding and those data points that were not considered in the fit. We next fixed a value for T_c and all the other parameters were least-squares adjusted. At this point T_c was released and the data fitted again.

For every fit we looked not only to rms deviation but also to the deviation plot, which is a plot of the difference between the fitted value and the measured one as a function of reduced temperature. Using these plots it was also possible to decide in a more accurate way which data points close to T_c were affected by the rounding. The fit was then repeated with a consequent improvement of its quality.

Next we tried to extend the temperature range including data that could be fitted with the same power law. We first fixed the t_{min} and increased t_{max} up to values where no changes were detected in the fit quality. The same procedure was then repeated fixing t_{max} and decreasing t_{min} to go as close as possible to T_c, looking for the widest temperature range where a single power law best represented the data and bearing in mind that a possible crossover could be expected for Cr_2O_3. Checks on the constraints on B and α were also made after t_{min} and t_{max} had been fixed. We first released the condition $\alpha=\alpha'$ but fits made for $T<T_c$ and $T>T_c$ gave values of the exponent which were equal within the errors. The same procedure and the same results were obtained when releasing the constraint $B=B'$. These checks also proved some prediction of the Renormalization Group Theory.

Finally, we add the correction to scaling term to our fitting function to check for an increase of the temperature range where the data can be fitted by the same power law. In this case we put the constraint $x=0.5$. The statistical errors for each parameter were calculated as the quantity which produce a variation of one standard deviation in the function which had to be minimized, adjusting all the other parameters to their best values. The function we minimized was a χ^2-like function and the uncertainty in the case of specific heat was 0.08%, while for the thermal diffusivity it was 0.04%.

The same fitting procedure was also used for the thermal diffusivity. In this case we did not put any constraint on b.

C. Results

1. *Specific heat*

The results of the fits for the specific heat are reported in Table I and the corresponding deviation plots are shown in Fig. 6. Fit 1 has been obtained with $D=D'=0$, $B=B'$, and $t_{max}=5\times10^{-3}$.

The fit quality is not very good as can be seen from the deviation plot of Fig. 6(a). A systematic deviation is evident near $t=10^{-3}$ and the t_{min} values of this fit are larger than the ones of any other fit. A further reduction of t_{max} gave a fit which was valid over less than one decade in reduced temperature. Moreover, the values of the critical exponent $\alpha=-0.043\pm0.006$ and of the amplitude ratio

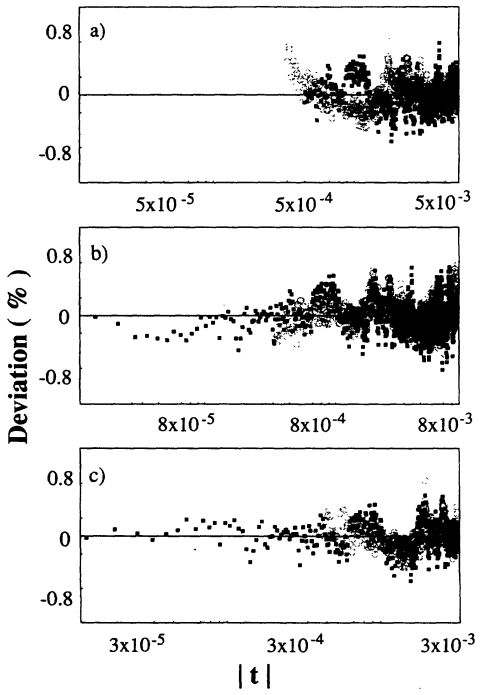

FIG. 6. Deviation plots corresponding to fits of Table I with $D=D'=0$: (a) Fit 1 with $B=B'$; (b) Fit 2; and (c) Fit 4 with $B\neq B'$.

TABLE II. Results of the fit for the specific heat with the correction to scaling factor included in the fitting function.

	Fit 5	Fit 6	Fit 7
t_{max}	8×10^{-3}	5×10^{-3}	3×10^{-3}
t_{min} $(T<T_c)$	3.4×10^{-4}	3.1×10^{-4}	3×10^{-4}
t_{min} $(T>T_c)$	6.5×10^{-6}	4.6×10^{-7}	6×10^{-6}
T_c (K)	307.249±0.025	307.245±0.025	307.257±0.015
α	−0.032±0.006	−0.032±0.007	0.10±0.02
A' (J/gK)	$(-4.8\pm0.1)\times10^{-1}$	$(-5.8\pm0.1)\times10^{-1}$	$(1.7\pm0.1)\times10^{-1}$
A (J/gK)	$(-6.3\pm0.1)\times10^{-1}$	$(-7.2\pm0.1)\times10^{-1}$	$(8.1\pm0.9)\times10^{-2}$
E (J/gK)	$(-1.8\pm0.4)\times10^{-2}$	$(-1.9\pm0.4)\times10^{-2}$	$(-3.3\pm0.9)\times10^{-4}$
B (J/gK)	1.46±0.01	1.55±0.01	$(7.9\pm0.1)\times10^{-1}$
D'	$(1.2\pm0.5)\times10^{-1}$	$(8.8\pm2.9)\times10^{-2}$	$(-1.9\pm0.9)\times10^{-1}$
D	$(-5.4\pm2.6)\times10^{-2}$	$(-6.0\pm2.0)\times10^{-2}$	$(-2.2\pm0.9)\times10^{-1}$
A/A'	1.25±0.05	1.25±0.04	0.48±0.08
rms	0.00177	0.00152	0.00147

$A/A'=1.20\pm0.05$ do not agree with any theoretical prediction.

Following the procedure of Ref. 2, we next allowed a discontinuity in the specific heat at T_c ($B\neq B'$), with $D=D'=0$. The fit quality improved as shown in the deviation plot reported in Fig. 6(b). Moreover, the fit is valid over a wider reduced temperature range. The results (Fit 2) are very similar to those obtained in Ref. 2: though $\alpha=-0.12\pm0.05$ is not too far from the Heisenberg behavior, the $A/A'=0.43\pm0.03$ is in strong disagreement with the theoretical predictions. For the Heisenberg system we expect $\alpha=-0.115\pm0.009$ and $A/A'=1.52\pm0.02$ (Ref. 16). Fits 3 and 4 have been obtained with $t_{max}=5\times10^{-3}$ and $t_{max}=3\times10^{-3}$, respectively.

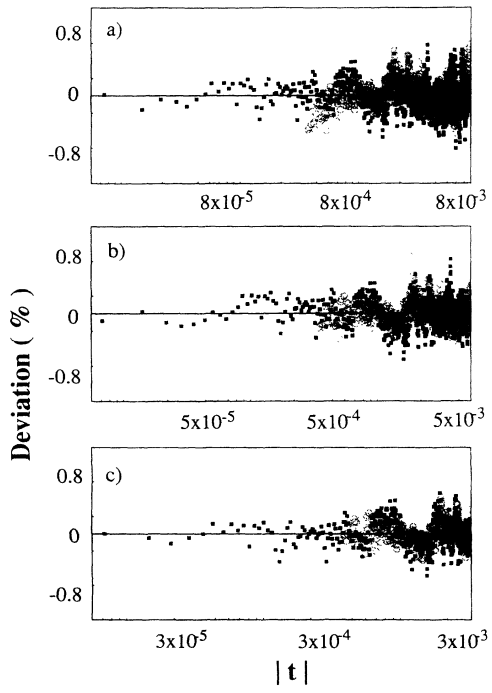

FIG. 7. Deviation plots corresponding to fits of Table II with $B=B'$, $D\neq D'\neq0$: (a) Fit 5; (b) Fit 6; and (c) Fit 7.

The deviation plots of Fits 2 and 4 are reported in Figs. 6(b) and 6(c), respectively. The disagreement with Heisenberg predictions becomes more evident mainly in the critical exponent which increases. No agreement with any other model can, however, be found.

Next we tried with $D\neq D'\neq0$ and $B=B'$; the results of these fits are reported in Table II, while the corresponding deviation plots are shown in Fig. 7. Fit 5 shows the results we have obtained for $t_{max}=8\times10^{-3}$.

It is clearly evident from the deviation plot shown in Fig. 7(a) that the fit quality is rather good and the rms deviation value is about the same of Fig. 2. Nevertheless, the values $\alpha=-0.032\pm0.006$ and $A/A'=1.25\pm0.05$ seem to indicate a nonuniversal behavior. Since, as stated earlier on, there is a possibility of a crossover for this material from Heisenberg to Ising very close to T_c, we tried to reduce t_{max}. Fit 6 shows the values we obtained for $t_{max}=5\times10^{-3}$ and the deviation plot is shown in Fig. 7(b). Again, no universal behavior can be recognized.

If t_{max} is further reduced to $t_{max}=3\times10^{-3}$ a strong indication of an Ising-like behavior, for which $\alpha=0.110\pm0.0045$ and $A/A'=0.51$ (Ref. 17) are expected, was found. Fit 7 shows these results where $\alpha=0.10\pm0.02$ and $A/A'=0.48\pm0.08$, while the corresponding deviation plot is reported in Fig. 7(c). Fit 7, which is shown in Fig. 8 with experimental data points

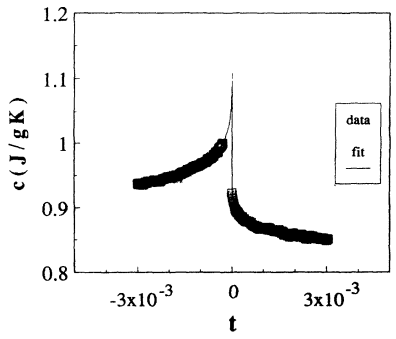

FIG. 8. Specific-heat data vs reduced temperature. Symbols are much larger than the experimental errors (see text). The solid line corresponds to Fit 7 of Table II.

close to T_c, is the one which allows the lowest values of t_{min} on both sides of T_c. To check if the abrupt change in α between Fits 6 and 7 of Table II can be due to the existence of two similar least-square minima, we made fits with α fixed. With $\alpha=0.10$ and the same t_{max} and t_{min} of Fig. 6, we found a fit with a rms=0.00176, which is larger than the one of Fig. 6 and a deviation plot shown in Fig. 9(a) which shows systematic deviation close to T_c. On the other hand, fixing $\alpha=-0.032$ and the same t_{max} and t_{min} of Fit 7, we found a fit with rms=0.00187 which is larger than the one of Fit 7 and, again, the deviation plot, shown in Fig. 9(b), clearly shows systematic deviation close to T_c. These results seem to suggest that while the data close to T_c can be described with an Ising-like behavior, a crossover to Heisenberg is present if t_{max} is increased.

The data points not included in the fit lie in a temperature interval of 96 mK around T_c. We do not have sufficient information to decide whether this "rounding" is due to the sample imperfections and impurities or to thermal gradients introduced by the measuring technique. Nevertheless, we are inclined, by our experience on the study of liquid crystal phase transitions,[18] which have been studied with the same experimental setup, to conclude that the thermal gradients due to the experimental setup play a role in a temperature region smaller than 20 mK around T_c. On the other hand, crystal imperfections do not seem to be relevant as shown in Fig. 3, so we can argue that the "rounding" is mainly due to impurities, even if it is not clear why t_{min} for $T<T_c$ is much smaller than t_{min} for $T>T_c$.

We can conclude from the above-mentioned results that the introduction of a discontinuity at T_c or, alternatively, of a correction to the scaling term, improves the fit quality, but, while in the second case there is strong evidence of an Ising-like behavior close to T_c, in the first case the results agree neither with Ising nor with Heisenberg model predictions.

2. *Thermal diffusivity*

The results of the fits for the thermal diffusivity are reported in Table III and the corresponding deviation plots are shown in Fig. 10. Fit 1 was obtained with $F=F'=0$ and $V=V'$. The rms deviation for this fit is smaller than

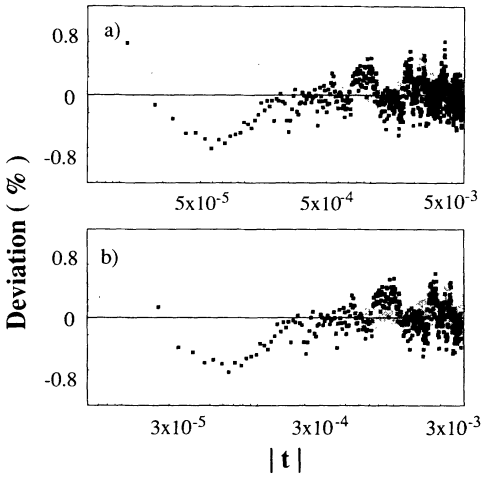

FIG. 9. Deviation plots corresponding to fit of the specific-heat data: (a) α fixed to 0.10—same t range of Fit 6 of Table II; (b) α fixed to -0.032-same t range of Fit 7 of Table II.

the corresponding value of our best fit for the specific heat (cf. Fit 6 of Table II) but we must be careful in the comparison of these two values. Thermal diffusivity data are much less scattered than the specific-heat ones as can be seen from the comparison of Figs. 3 and 5. For this reason we expect a larger rms deviation for the best fit of the specific heat than the corresponding one of the thermal diffusivity. As a matter of fact, if we look at the deviation plot corresponding to Fit 1 of Table III reported in Fig. 10(a), a systematic deviation close to T_c is clearly evident.

Further reduction of t_{max} gave fits valid over less than one decade and we did not consider them. So we next allowed a discontinuity ($V\neq V'$) at T_c also in the case of thermal diffusivity. Discontinuities in D have been reported in literature for several liquid-crystal phase transitions and no explanation was available until now.[4]

Fit 2 shows the results we have obtained for $t_{max}=8\times10^{-3}$. The rms deviation value we obtained is close to the one of Fit 1 and the deviation plot, reported in Fig. 10(b), continues to shows systematic deviations close to T_c.

Improvements have been obtained decreasing t_{max} to

TABLE III. Results of the fit for thermal diffusivity data with no correction term.

	Fit 1	Fit 2	Fit 3	Fit 4
t_{max}	5×10^{-3}	8×10^{-3}	5×10^{-3}	3×10^{-3}
t_{min} $(T<T_c)$	1.6×10^{-4}	2×10^{-4}	1.9×10^{-4}	3×10^{-4}
t_{min} $(T>T_c)$	5.7×10^{-4}	3.5×10^{-4}	3.4×10^{-4}	1.4×10^{-5}
T_c (K)	307.136±0.02	307.176±0.015	307.181±0.015	307.254±0.015
b	−0.18±0.03	−0.27±0.03	−0.26±0.03	−0.09±0.02
U' (cm²/s)	$(3.2\pm0.5)\times10^{-3}$	$(3.3\pm0.6)\times10^{-3}$	$(-3.4\pm0.7)\times10^{-3}$	$(-1.26\pm0.09)\times10^{-2}$
U (cm²/s)	$(6.5\pm0.5)\times10^{-3}$	$(3.5\pm0.4)\times10^{-3}$	$(-3.5\pm0.6)\times10^{-3}$	$(-5.5\pm0.7)\times10^{-3}$
W (cm²/s)	$(-6.6\pm0.6)\times10^{-4}$	$(-3.5\pm0.8)\times10^{-4}$	$(-3.0\pm1)\times10^{-4}$	$(2.8\pm2.4)\times10^{-5}$
V' (cm²/s)	$(2.47\pm0.05)\times10^{-2}$	$(2.48\pm0.06)\times10^{-2}$	$(2.45\pm0.09)\times10^{-2}$	$(1.61\pm0.09)\times10^{-2}$
V (cm²/s)	$(2.47\pm0.05)\times10^{-2}$	$(2.74\pm0.04)\times10^{-2}$	$(2.74\pm0.09)\times10^{-2}$	$(2.50\pm0.09)\times10^{-2}$
U/U'	2.03±0.47	1.06±0.31	1.03±0.37	0.44±0.08
rms	0.00076	0.00050	0.00044	0.00051

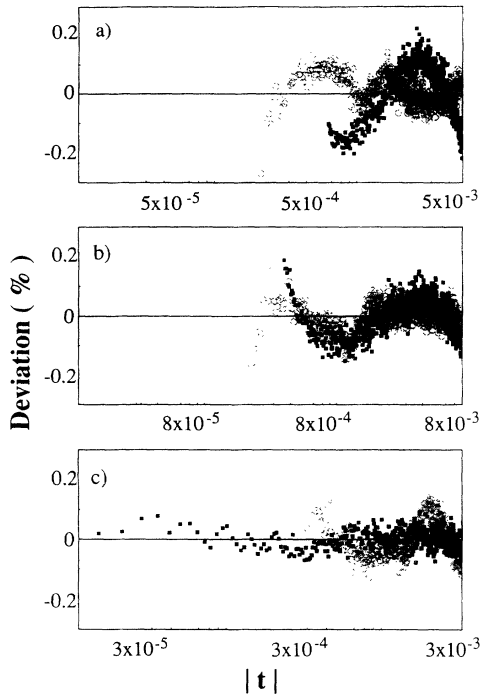

FIG. 10. Deviation plots corresponding to fits of Table III with $F=F'=0$: (a) Fit 1 with $V=V'$; (b) Fit 2 and (c) Fit 4 with $V\neq V'$.

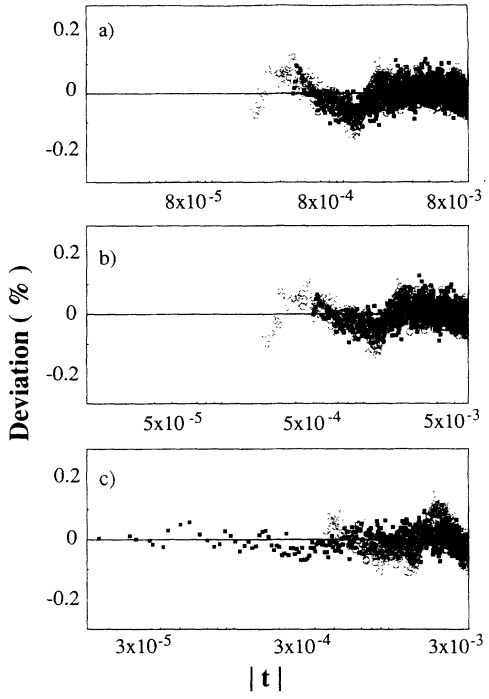

FIG. 11. Deviation plots corresponding to fits of Table IV with $V=V'$ and $F\neq F'\neq 0$: (a) Fit 5; (b) Fit 6; and (c) Fit 7*.

5×10^{-3} and 3×10^{-3}, respectively, as can be seen from Fits 3 and 4. The deviation plot of Fit 4 is shown in Fig. 10(c).

Table IV shows the results we obtain setting $F\neq F'\neq 0$ and $V=V'$. The deviation plot corresponding to Fit 5, reported in Fig. 11(a) which has been obtained with $t_{\max}=8\times10^{-3}$, shows rather small systematic deviation. Though this fit seems statistically acceptable, we tried to reduce $t_{\max}$ to investigate the possibility of a crossover. Fit 6 corresponds to $t_{\max}=5\times10^{-3}$. No significant variations are evident in the rms value but also in the deviation plot which remains quite good as can be seen from Fig. 11(b).

For $t_{\max}=3\times10^{-3}$ the best fit (not reported in Table IV) was obtained with a positive b value. This fit is not acceptable since a positive b does not give the right asymptotic behavior for D which is expected to remain finite as T approaches T_c.

Assuming a nonsingular behavior for k (cf. Fig. 4) and since $D=k/\rho c_p$, we tried to fit the data in this interval with the function

$$D=\frac{V+W(T-T_c)}{1+U|T-T_c|^b(1+F|T-T_c|^{0.5})} \quad (\text{with } b<0)\,, \tag{6}$$

where the linear term in the denominator coming from the specific-heat expression has been neglected (cf. Fit 7

TABLE IV. Results of the fit for the thermal diffusivity with the correction to scaling factor included in the fitting function. Fits 5, 6, and 8 have been obtained using Eq. (5), while Fit 7* has been obtained using Eq. (6). The parameters in Fit 7* have different meanings and therefore different units with respect to the ones of the other fits (see text).

	Fit 5	Fit 6	Fit 7*	Fit 8
$t_{\max}$	8×10^{-3}	5×10^{-3}	3×10^{-3}	2.5×10^{-3}
$t_{\min}$ $(T<T_c)$	1.8×10^{-4}	1.8×10^{-4}	3×10^{-4}	3×10^{-4}
$t_{\min}$ $(T>T_c)$	3.8×10^{-4}	3.8×10^{-4}	2.5×10^{-5}	4.5×10^{-5}
T_c (K)	307.190±0.015	307.192±0.015	307.249±0.015	307.240±0.015
b	−0.015±0.002	−0.016±0.002	−0.11±0.02	−0.09±0.01
U' (cm^2/s)	$(2.47\pm0.2)\times10^{-2}$	$(2.50\pm0.2)\times10^{-2}$	$(2.00\pm0.05)\times10^{-1}$	$(6.5\pm0.3)\times10^{-3}$
U (cm^2/s)	$(2.76\pm0.2)\times10^{-2}$	$(2.80\pm0.2)\times10^{-2}$	$(8.3\pm0.6)\times10^{-2}$	$(1.27\pm0.04)\times10^{-2}$
W (cm^2/s)	$(-2.8\pm1.5)\times10^{-4}$	$(-3.0\pm1.5)\times10^{-4}$	$(-5\pm5)\times10^{-6}$	$(2.6\pm0.8)\times10^{-3}$
V (cm^{2}s)	$(2.35\pm0.01)\times10^{-3}$	$(2.13\pm0.01)\times10^{-3}$	$(3.24\pm0.05)\times10^{-2}$	$(2.02\pm0.01)\times10^{-2}$
F'	$(4.8\pm0.5)\times10^{-2}$	$(4.3\pm0.5)\times10^{-2}$	$(-2.9\pm1.5)\times10^{-1}$	$(6\pm1)\times10^{-1}$
F	$(3.0\pm0.5)\times10^{-2}$	$(2.7\pm0.5)\times10^{-2}$	$(-2.7\pm1.5)\times10^{-1}$	$(-3.8\pm0.5)\times10^{-1}$
U/U'	1.12±0.17	1.12±0.17	0.42±0.04	1.95±0.08
rms	0.00041	0.00039	0.00047	0.00034

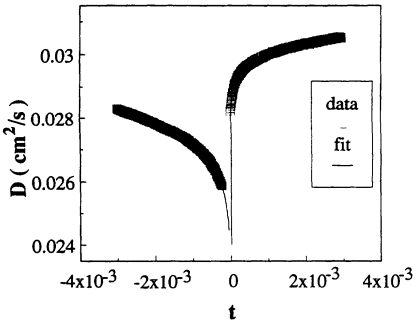

FIG. 12. Thermal diffusivity data vs reduced temperature. Symbols are much larger than the experimental errors (see text). The solid line corresponds to Fit 7 of Table IV.

Table II). It should be noted that even if, for the sake of simplicity, we used the symbols for the parameters V, W, U, and F in Eq. (6) and for Fit 7 of Table IV, they have different meanings and different units with respect to the ones of Eq. (5). The obtained results correspond to Fit 7.

Both the rms value and the deviation plot shown in Fig. 11(c) demonstrate the good quality of the fit. A good fit, with a deviation plot (not shown) similar to the one of Fig. 11(c), also can be obtained using Eq. (5) as fitting function and putting a constraint on b which was not allowed to be positive. The results correspond to Fit 8.

Although this fit is valid in a narrower reduced temperature range, in this case we do not need make any assumption on the k behavior. It should be also noted that Fits 7 and 8 have approximately the same critical exponent which is also very close in modulus to the one of Fit 7 of Table II. Figure 12 shows the diffusivity data compared with Fit 7.

VI. DISCUSSION

A. Specific heat

As far as we know, the only high-resolution data available on the critical behavior of the specific heat of Cr_2O_3 are the ones reported in Ref. 2. In that case the obtained result for the critical exponent was -0.12 ± 0.03, which is quite close the theoretical prediction for a Heisenberg model. The authors, however, pointed out that behind this value of the critical exponent there were, in the results of the fit, at least two points which could not be explained. They were not able to fit the data without a discontinuity in c at T_c ($B\neq B'$) and obtained an amplitude ratio $A/A'=0.56$, which is much smaller than the value of 1.52 ± 0.02 expected in 3D for the Heisenberg universality class in the second-order ε expansion.[16] They suggested an explanation for this apparent nonuniversal behavior of the specific-heat data which was based on a possible systematic error present in the measurement due to the difference between c_p (measured value) and c_v (theoretical prediction). The Heisenberg behavior was, therefore, neither confirmed nor excluded for Cr_2O_3. The authors also argue that the presence of such a systematic error can be a severe limit whenever a comparison between theory and experiment is attempted. To check this hypothesis, a detailed knowledge of the expansion coefficient and of the elastic constants of the material, which allow an estimation of c_p-c_v together with very high-quality materials, to go closer to T_c, are required.

The results reported in Table I (cf. Fit 2) are essentially consistent with the ones reported in Ref. 2. A good fit can be obtained only if a discontinuity at T_c is allowed in the specific heat. The results of this fit, however, can be explained neither with a Heisenberg behavior nor with an Ising one. On the other hand, Fit 7 of Table II, which has been obtained with the introduction of a correction to scaling factor, seems to support an Ising-like behavior, since the critical exponent was $\alpha=0.10\pm0.02$ and $A/A'=0.48\pm0.03$. It should be noted that the fits in Ref. 2 have been performed including about 27 points on each side of T_c, while Fit 7 of Table II has been calculated over more than 400 points on each side. This is probably the reason why the correction to scaling term in the data analysis of Ref. 2 gave no effect.

B. Thermal diffusivity and thermal conductivity

The dynamic models corresponding to Heisenberg and Ising behavior for an antiferromagnet are essentially based on the presence in the Hamiltonian of terms which can allow or not allow its invariance under rotation of the axis of spin quantization. If this invariance is allowed, then we have the so-called "isotropic" antiferromagnet model, which is the dynamic analog of the Heisenberg model in statics, whose thermal conductivity is expected to diverge at T_c.[19] This is not the case of the k data reported in Fig. 4, which do not show any divergence at the transition temperature. On the other hand, the specific-heat data seem to suggest an Ising-like behavior very close to T_c. Let us now derive what we have to expect for D in the case of an anisotropic antiferromagnet with $n=1$. The only conserved quantity in this case can be the energy E since the order parameter, which represents the staggered magnetization, is not conserved. In real systems, energy conservation depends on the rate of energy transfer from the spins to phonons; if this rate is slow compared to the spins exchange frequencies, then we can consider the spin system as thermally isolated (model C). If this is not true, the system is better described by a model with no energy conservation (model A). One of the consequences of the conservation of energy is that the heat conduction mode is purely diffusive.[20]

Assuming that the dynamic scaling hypothesis is applicable to the energy (extended scaling[21]), it has been shown[20] that for model C $\omega_E=iDq^2\propto q^{z_E}$ where q is the mode wave vector, $z_E=2+\tilde{\alpha}/\nu$, and $\tilde{\alpha}=\max(\alpha,0)$. Now, since $D\propto\Delta T^{-b}$, we obtain

$$\omega_E=iDq^2\propto\xi^{b/\nu}q^2=(q\xi)^{b/\nu}q^{2-b/\nu},$$

where ξ is the correlation length and therefore $z_E=2-b/\nu$. This means that for model C we have to expect $-b\sim\alpha$. RG calculations have shown[20] that, for model A in the region where c diverges, the nonconserved energy relaxes with the same exponent of the order parameter $z_E=2+c\eta$, where $c=0.726(1-1.69\varepsilon$

$+\cdots$). All this demonstrates the usefulness of the measurement of the critical behavior of c and D to clearly establish the universality class to which the system belongs, particularly if the measurements are made simultaneously under the same experimental conditions and with the same sample.

It is evident looking at the deviation plots reported in Fig. 10(a) that good fits cannot be obtained with the constraints $V=V'$ and $F=F'=0$. It is also evident that in the case of the thermal diffusivity, the introduction of a discontinuity at T_c ($V\neq V'$) gave no substantial improvements in the fit for $|t|\leq 8\times 10^{-3}$ [cf. Fig. 10(b)]. This was not the case of the specific heat where the release of the constraint $B=B'$ led to an improvement in the fit quality for $|t|\leq 8\times 10^{-3}$, though no agreement with theoretical predictions was found. As already stated, however, the comparison of the deviation plot of Fig. 6(b) with the one of Fig. 10(b) can be misleading since the uncertainty of the specific-heat data is larger than the one of the thermal diffusivity ones. We can therefore conclude that the fits on the thermal diffusivity are, in general, more "reliable" than the ones for the specific heat, as can also be seen from the errors in parameters.

Now, while in the case of the specific heat, good fits over wide temperature ranges were obtained either with a discontinuity at T_c or with a correction to the scaling factor, in the case of thermal diffusivity a good fit valid for $|t|\leq 8\times 10^{-3}$ can be obtained only if a correction term is included in the fitting function. It is also interesting to note that both Fits 7 and 8 of Table IV show that $-b\sim\alpha$, in agreement with what is expected for the model C which is valid for a uniaxial antiferromagnet. This conclusion is also consistent with the one we have drawn from Fit 7 of Table II.

It is well known that anisotropy fields can be due to mechanical stresses. The results we got for c, k, and D for the annealed sample seem to rule out this possibility for Cr_2O_3. Regarding the purity, it seems to be larger than the one of the sample used in Ref. 2 since the transition temperature is about 0.1 K higher. Even if no comparison is possible with samples used in other experiments, we think that the $3N$ purity of our sample is close to the best attainable value. Uniaxial behavior was, on the other hand, obtained very close to T_c ($t\leq 3\times 10^{-3}$) where an Ising-like behavior is expected even for a weak uniaxial antiferromagnet as Cr_2O_3

As stated earlier in our remarks on thermal conductivity, data are in qualitative agreement with the ones reported in Ref. 2 for temperatures away from the transition temperature. Close to T_c, however, a strong disagreement has been found. Bruce and Cannel[2] reported a peak in k at T_c which was attributed to some experimental artifacts. Our data, on the contrary, clearly show a discontinuity whose origin is not completely understood at the moment. The approximately linear behavior with no anomaly, which we have found close to T_c (cf. the insert of Fig. 4), is consistent with the conclusions already drawn for c and D.

VII. CONCLUSIONS

We have used high-resolution photopyroelectric calorimetry to simultaneously measure the critical behavior of specific heat, thermal conductivity, and thermal diffusivity of Cr_2O_3 at the antiferromagnetic-paramagnetic phase transition. An Ising-like behavior has been found for $|t|\leq 3\times 10^{-3}$, while increasing t_{max} a crossover seems to appear. These results are confirmed by the thermal diffusivity data, which can be fitted in the same reduced temperature range of the specific heat according to a model for an uniaxial antiferromagnet with energy conservation.

To check for possible mechanical stress induced anisotropy we annealed one sample, but no significant variations have been detected in the critical behavior. No anomaly has been found in the thermal conductivity, where a small discontinuity is present at T_c.

The k behavior is approximately linearly dependent upon T with a change in slope at T_c. This result is consistent with the ones obtained for the specific heat and the thermal diffusivity which have the approximately same critical exponent with different sign, thus not suggesting an anomaly at T_c.

ACKNOWLEDGMENTS

This work has been partially supported by INFM and CNR.

*Author to whom correspondence should be sent.

[1]G. Ahlers and A. Kornblitt, Phys. Rev. B **12**, 1938 (1975).
[2]R. H. Bruce and D. S. Cannell, Phys. Rev. B **15**, 4451 (1977).
[3]G. Ahlers, Phys. Rev. Lett. **21**, 1159 (1968); S. M. Bhagat and R. A. Lasken, Phys. Rev. A **3**, 340 (1971).
[4]E. K. Hobbie and C. C. Huang, Phys. Rev. A **39**, 4154 (1989).
[5]J. Samuelson, M. T. Hutchings, and G. Shirane, Physica **48**, 13 (1970).
[6]S. Foner, Phys. Rev. **130**, 183 (1963).
[7]T. Riste and A. Wanic, Phys. Lett. **16**, 231 (1965).
[8]A. Bachellerie and C. H. Frenois, J. Phys. (Paris) **35**, 30 (1974).
[9]M. Marinelli, U. Zammit, F. Mercuri, and R. Pizzoferrato, J. Appl. Phys. **72**, 1096 (1992).
[10]A. Mandelis and M. Zver, J. Appl. Phys. **57**, 4421 (1985).
[11]S. Greenwald, Nature **168**, 379 (1951).
[12]A. M. Glass, Phys. Rev. **172**, 564 (1968).
[13]G. Ahlers, Rev. Mod. Phys. **52**, 489 (1980).
[14]A. Aharony and M. E. Fisher, Phys. Rev. B **27**, 4394 (1983).
[15]B. I. Halperin, P. C. Hohenberg, and E. D. Siggia, Phys. Rev. B **13**, 1299 (1976).
[16]A. Aharony and A. D. Bruce, Phys. Rev. B **10**, 2973 (1974).
[17]A. Aharony and P. C. Hohenberg, Phys. Rev. B **13**, 3081 (1976); J. C. Le Guillou and J. Zinn-Justin, *ibid.* **21**, 3976 (1980).
[18]U. Zammit, M. Marinelli, R. Pizzoferrato, F. Scudieri, and S. Martellucci, Phys. Rev. A **41**, 1153 (1990).
[19]P. C. Hohenberg and B. I. Halperin, Rev. Mod. Phys. **49**, 435 (1977).
[20]B. I. Halperin, P. C. Hohenberg, and S. Ma, Phys. Rev. B **10**, 139 (1974).
[21]B. I. Halperin and P. C. Hohenberg, Phys. Rev. **177**, 952 (1969).